Precision Control and Simulation Verification of Hydraulic Manipulator under Unknown Load

Qixian Wang [#], Manzhi Qi [#], Yangxiu Xia, Zheng Chen [*]

Ocean College, Zhejiang University, Zhoushan, Zhejiang, 316021, China
qxwang_m@zju.edu.cn,manzhi.q@zju.edu.cn,yx.xia@zju.edu.cn
zheng_chen@zju.edu.cn

Abstract. Hydraulic manipulators with multiple degrees of freedom have an increasing range of applications in industrial production, and have the potential to complete various complex tasks. Nowadays, the complex and precision-demanding working environment often requires the hydraulic manipulators to have high control accuracy, which limits their usage. The inherent high-order nonlinearity and uncertainty of hydraulic systems greatly affect the precise control of hydraulic manipulators. High order dynamics such as friction and vibration also have a significant impact on their controlling. Additionally, manipulator typically operates in complex environments with large loads, the end load has always been an important external factor affecting their control accuracy. In this paper, a direct/indirect adaptive robust controller (DIARC) is developed. By incorporating nonlinear and uncertain terms into the dynamic modeling, the control accuracy can be improved. In addition, the end load of the manipulator is incorporated into the parameter space, which makes end load estimation possible. Simulation is constructed using MATLAB Simscape and the performance of the controller is attested. Results shows that the controller can not only improve the tracking accuracy when the end load is heavy, but precisely identify the mass of end load precisely.

Keywords: Hydraulic manipulator, Adaptive robust control, End load estimation.

1 Introduction

Hydraulic manipulator with multiple degrees of freedom (DOF), as the combination of hydraulic system and automation technology, has been increasingly used. They enjoy many advantages such as convenient maintenance and strong load-bearing capacity. However, with the development of industrial intelligence, the complexity of tasks is increasing and the required operational accuracy is improving, which to some extent limits the application of hydraulic manipulators due to their lack of control accuracy.

The main reason for the limited application of hydraulic manipulators is the lack of control accuracy. Nowadays, most hydraulic manipulators are open-loop operated, and closed-loop control often uses PID controller. Due to the influence of the manipulator

[#] These authors contributed equally to this work
[*] Corresponding author

flexibility, vibration, inter-joint clearance, combined friction and temperature inside the hydraulic cylinder, complex external interference and so on, it is difficult to effectively improve control accuracy [1,2].

In order to pursue more accurate control, Yao *et al* combined the RISE-based controller with parameter adaptive control to decrease the system tracking error, which can effectively suppress parameter uncertainty and reduce tracking error of hydraulic system [3,4]. Xia estimated the viscous friction coefficient and coulomb friction coefficient of hydraulic system, and achieved high tracking accuracy [5]. However, the experimental object of the above methods is hydraulic single push rod, and the effect on the manipulator still needs to be verified. In recent years, research on hydraulic manipulators has gradually deepened. Mattila *et al*. proposed virtual decomposition control (VDC) control method, which achieved impressive effect on multi-DOF hydraulic manipulator [6,7]. And many scholars have studied the influence of various environmental parameters and mechanical structure parameters on the performance of hydraulic manipulator, and proposed different kinds of controllers [8-11]. However, these studies mainly focus on laboratory environments. In actual production, hydraulic manipulators often face complex time-varying loads.

The end load is also an important factor that seriously affects the accuracy and control effect of operations. But in many engineering tasks, such as excavation and logging, the idea of using a force/torque sensor at the end-effector is difficult due to the nature of the contact task [12]. Therefore, designing a specific control law for load estimation is a practical and feasible solution. The load variation of the end-effector on electric rigid manipulator were studied. Duan *et al*. proposed a variable structure robust control method with feedforward compensator based on equivalent control for robots with load uncertainty, which can adapt to end-load changes under the condition of powerless sensors and achieve better control effect [13]. Scholars like Zeng *et al* also discussed the method of estimating load conditions for electric rigid body robots [14,15]. However, most of the above research focuses on industrial robots, there is still little research on load estimation of hydraulic manipulators with more complex dynamic characteristics.

In this paper, to achieve precise control under unknown loads, a direct/indirect adaptive robust controller (DIARC) focusing on the time-varying end load is proposed. The controller overcomes the nonlinearity and uncertainty of hydraulic systems and can achieve considerable improvement in tracking accuracy. It also incorporates end-load into the dynamic system to achieve accurate estimation of end load. The load will be integrated into the control law afterwards, further improving the control effect under variable and unknown loads. Finally, simulation is conducted to attest the tracking accuracy and end load estimation precision. The new method is expected to be applied to goods sorting, construction engineering, mining and other industries which have high requirements for load recognition.

2 Problem formulation

2.1 Dynamic modeling

The hydraulic manipulator analyzed in this article is a two DOF manipulator. Only the swing joint which is connected to the base and the wrist joint at the end will be considered. Fig.1 shows the structure diagram of the manipulator and identified the controlled joints.

Supposing the centroid is at the center of each rod, the dynamic model of a manipulator is established using the Lagrange method and described as follows,

$$H(q)\ddot{q}+C(q,\dot{q})\dot{q}+G(q)+f_1 s(\dot{q})+f_2\dot{q}=T+\Omega_1 \tag{1}$$

where q_1 and q_2 are the angle of swing joint and wrist joint, respectively, $H(q)\in\mathbb{R}^{2\times2}$ is the mass matrix, $C(q,\dot{q})\in\mathbb{R}^{2\times2}$ the matrix of inertia, $G(q)\in\mathbb{R}^{2\times1}$ the matrix of gravity, $f_1=diag(f_{v1},f_{v2})$ the viscous friction matrix and $f_2=diag(f_{c1},f_{c2})$ the coulomb friction matrix, $s(\dot{q})=2\arctan(900\dot{q})/\pi$, $T\in\mathbb{R}^2$ the matrix of torque, $\Omega_1\in\mathbb{R}^2$ the modeling uncertainty. $H(q)$, $C(q,\dot{q})$ and $G(q)^T$ can be expressed as Eq.2, Eq.3 and Eq.4, respectively.

$$H(q)=\begin{pmatrix}(L_1m_2+L_1m_t+L_2m_t\cos(q_2))(L_1+L_2\cos(q_2)) & 0\\ 0 & J+L_2^2m_t\end{pmatrix} \tag{2}$$

$$C(q,\dot{q})=\begin{pmatrix}-\frac{1}{2}L_2\dot{q}_2x & -\frac{1}{2}L_2\dot{q}_1x\\ \frac{1}{2}L_2\dot{q}_1x & 0\end{pmatrix},\ x=\sin(2q_2)L_2m_t+L_1\sin(q_2)(m_2+2m_t) \tag{3}$$

$$G(q)^T=\left(0,\frac{1}{2}gL_2\cos(q_2)(m_2+2m_t)\right) \tag{4}$$

where L_i (i=1.2) is the length of the two arms, $J_t=L_2^2m_t$, J is the moment of the wrist arm, m_t is the mass of the end load, m_2 the mass of wrist arm. The hydraulic dynamics of a manipulator are expressed in the following form,

$$\frac{V_1}{\beta_e}\dot{p}_1=A_1\frac{\partial X_L}{\partial q}\dot{q}+Q_1+\Omega_2,\ \frac{V_2}{\beta_e}\dot{p}_2=A_2\frac{\partial X_L}{\partial q}\dot{q}-Q_2+\Omega_3 \tag{5}$$

where $V_1\in\mathbb{R}^{2\times2}$ and $V_2\in\mathbb{R}^{2\times2}$ are the volume matrixes of the chambers, $A_1\in\mathbb{R}^{2\times2}$ and $A_2\in\mathbb{R}^{2\times2}$ the area matrixes of the chambers. $\frac{\partial X_L}{\partial q}=diag(\frac{\partial x_1}{\partial q_1},\frac{\partial x_2}{\partial q_2})$ can be used to

represent the driving force arm of the joints. $Q_1 \in \mathbb{R}^2$ is the input flow matrix and $Q_2 \in \mathbb{R}^2$ is the return flow matrix. Based on Eq.5, the control force can be written as,

$$\begin{aligned} F_L &= P_1 A_1 - P_2 A_2 \\ \vartheta_8 \dot{F}_L &= \vartheta_8 (\dot{P}_1 A_1 - \dot{P}_2 A_2) = -\lambda_A \cdot \frac{\partial X_L}{\partial q} \cdot \dot{q} + Q_L + \lambda_B \Omega_2 + \lambda_C \Omega_3 \end{aligned} \tag{6}$$

where $\lambda_A = diag(\lambda_{A1}, \lambda_{A2})$, $\lambda_B = diag(\lambda_{B1}, \lambda_{B2})$ and $\lambda_C = diag(\lambda_{C1}, \lambda_{C2})$ are used to facilitate equation expression and $Q_L \in \mathbb{R}^2$ is the control flow.

Then, the relation between the control flow and the valve input voltage can be expressed as,

$$Q_L = k_v u \sqrt{\Delta p} \tag{7}$$

where k_v is the conversion coefficient, $u = diag(u_1, u_2)$ the matrix of valve input voltage and $\sqrt{\Delta p} \in \mathbb{R}^2$ the matrix of pressure difference of the valve ports.

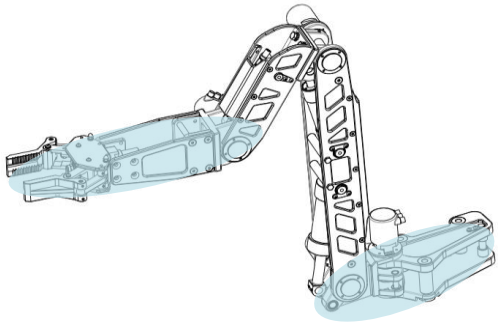

Fig. 1. Structure diagram of the hydraulic manipulator

2.2 Parameterization of dynamic models

Eq.1 can be further written in the form of a regression matrix as,

$$T = \frac{\partial X_L}{\partial q} F_L = \phi_1^T \vartheta \tag{8}$$

where ϑ is the matrix of uncertain parameters. ϑ can be expressed in the following form,

$$\vartheta = [\vartheta_1, \vartheta_2, \vartheta_3, \vartheta_4, \vartheta_5, \vartheta_6, \vartheta_7, \vartheta_8, \vartheta_9, \vartheta_{10}, \vartheta_{11}, \vartheta_{12}, \vartheta_{13}, \vartheta_{14}]^T \tag{9}$$

$$\vartheta = [m_t, J, m_2, F_{v1}, F_{v2}, F_{s1}, F_{s2}, \frac{1}{\beta_e}, \bar{\Omega}_{11}, \bar{\Omega}_{12}, \bar{\Omega}_{21}, \bar{\Omega}_{22}, \bar{\Omega}_{31}, \bar{\Omega}_{32}]^T \tag{10}$$

where $\bar{\Omega}_i, i=1,2,3$ is the calculable parts of Ω_i . At this point, the parameterization of the dynamic models is complete, it is clear that m_t has been parameterized separately.

Subsequently, the main aim is designing a virtual control flow Q_{Ld} so that an appropriate valve input voltage can be generated to drive the hydraulic system to track the given trajectory. Additionally, another aim is to propose an adaptation law to accurately estimate m_t .

3 Controller design

3.1 Basic DIARC controller construction

In this section, a DIARC controller is designed so that the precise control of the manipulator can be realized. The algorithm flow chart of the controller is shown in Fig.2. In the following parts of the paper, $\hat{\bullet}$ represent the estimation of $\bullet$, and $\tilde{\bullet}=\hat{\bullet}-\bullet$ is the error between the two values.

Step I

The angular error and the angular velocity error are defined as,

$$e_1 = q - q_d,\ e_2 = \dot{e}_1 + k_1 e_1 = \dot{q} - \dot{q}_{eq} \tag{11}$$

where $\dot{q}_{eq} = \dot{q}_d - k_1 e_1$ is the slip modulus and $k_1 \in \mathbb{R}^{2\times 2}$ a positive definite diagonal matrix. Similar to Eq.8, Eq.1 can be described with q_{eq} as Eq.12. Therefore, the difference between Eq.12 and Eq.1 can be written as Eq.13.

$$H(q)\ddot{q}_{eq} + C(q,\dot{q})\dot{q}_{eq} + G(q) + f_1 s(\dot{q}) + f_2\dot{q} = \phi_2^T \vartheta + \Omega_1 \tag{12}$$

$$H(q)\dot{e}_2 + C(q,\dot{q})e_2 = -\phi_2{}^T \vartheta + \frac{\partial X_L}{\partial q} F_L \tag{13}$$

Then a virtual control force used to replace F_L can be written as,

$$\begin{aligned} &F_{Ld} = F_{Lda} + F_{Lds},\ F_{Lda} = F_{Lda1} + F_{Lda2},\ F_{Lds} = F_{Lds1} + F_{Lds2} \\ &F_{Lda1} = \frac{\partial q}{\partial X_L}\varphi_2{}^T\hat{\theta},\ F_{Lds1} = -k_2 e_2 \frac{\partial q}{\partial X_L} \end{aligned} \tag{14}$$

where F_{Lda1} can compensate for nonlinear terms in dynamic equations, F_{Lds1} can ensure the error of tracking force converges exponentially if k_2 is a positive diagonal matrix. F_{Lda2} and F_{Lds2} are designed in the following step.

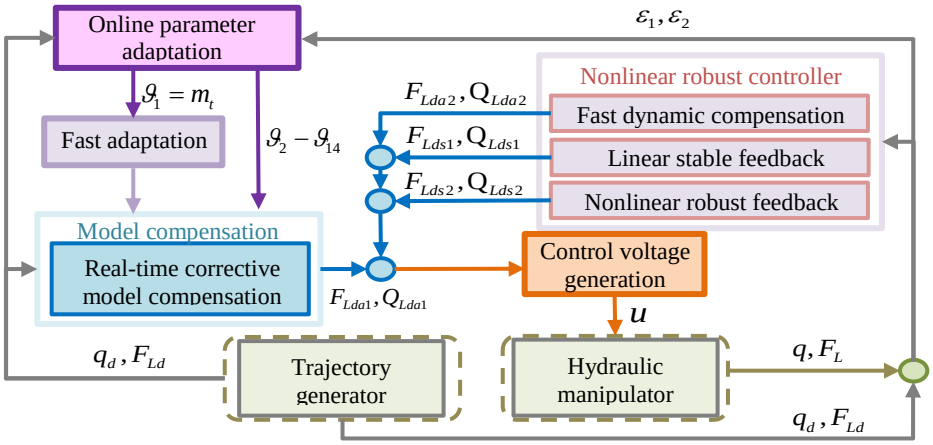

Fig. 2. Algorithm flow chart of the controller

Step II

The error between the real output force and the virtual output force is written as Eq.15, and its differentiation can be written as Eq.17.

$$e_3 = F_L - F_{Ld} \tag{15}$$

$$\dot{F}_{Ld} = \dot{F}_{Ldc} + \dot{F}_{Ldi},\ \dot{F}_{Ldc} = \frac{\partial F_{Ld}}{\partial q}\dot{q} + \frac{\partial F_{Ld}}{\partial \dot{q}}\hat{\dot{q}} + \frac{\partial F_{Ld}}{\partial t} \tag{16}$$

$$\begin{aligned} \vartheta_8 \dot{e}_3 &= \vartheta_8 \dot{F}_L - \vartheta_8 \dot{F}_{Ld} \\ &= \phi_3^T \vartheta + Q_L - \vartheta_8 \dot{F}_{Ldi} \end{aligned} \tag{17}$$

where $\dot{F}_{Ldc}$ and $\dot{F}_{Ldi}$ is the calculable part and incalculable part of $\dot{F}_{Ld}$ respectively. $\hat{\dot{q}} = \hat{H}(q)^{-1}(\frac{\partial X_L}{\partial q}F_{Ld} + \Omega_1 - \hat{C}(q,\dot{q})\dot{q} - \hat{G}(q) - \hat{f}_1 s(\dot{q}) - \hat{f}_2 q)$. ϕ_3^T is also a regression matrix.

In Eq.17, Q_L is substituted by the virtual control flow Q_{Ld} and can be expressed as,

$$\begin{aligned} &Q_{Ld} = Q_{Lda} + Q_{Lds},\ Q_{Lda} = Q_{Lda1} + Q_{Lda2},\ Q_{Lds} = Q_{Lds1} + Q_{Lds2} \\ &Q_{Lda1} = -\phi_3^T \hat{\vartheta} + \mu,\ Q_{Lds1} = -k_3 e_3 \end{aligned} \tag{18}$$

where $\mu = -\frac{\partial X_L}{\partial q}\frac{\omega_1}{\omega_2}e_2$ can be used to balance the order of magnitude of F_{Ld} and Q_{Ld}, so that they have the same effect in the controller. Q_{Lda1} can compensate for nonlinear

terms in hydraulic dynamic equations. Q_{Lds1} can ensure the error of control flow converges exponentially if k_3 is a positive diagonal matrix. The dynamic equations in Eq.13 and Eq.17 are expressed as follows,

$$\begin{aligned} H(q)\dot{e}_2 + C(q,\dot{q})e_2 &= -k_2 e_2 - \phi_2^T \tilde{\vartheta} + \frac{\partial X_L}{\partial q} e_3 + \frac{\partial X_L}{\partial q} F_{Lda2} \\ \vartheta_8 \dot{e}_3 &= -k_3 \mathrm{e}_3 - \phi_3^T \tilde{\vartheta} + Q_{Lda2} - \vartheta_7 \dot{F}_{Ldi} + \mu \end{aligned} \tag{19}$$

In Eq.19, the fast-dynamic compensation items are expressed as,

$$F_{Lda2} = -\frac{\partial q}{\partial X_L}\gamma_1,\ Q_{Lda2} = -\gamma_2 \tag{20}$$

where γ_1 is the low frequency part of $-\phi_2^T \tilde{\vartheta}$, γ_2 the low frequency part of $-\phi_3^T \tilde{\vartheta} - \vartheta_7 \dot{F}_{Ldi} + \mu$. They are updated by the following updating law,

$$\dot{\gamma}_i = \begin{cases} 0, & if\ |\hat{\gamma}_i| = \gamma_{iM}\ \ and\ \ \hat{\gamma}_i(t) e_{i+1} > 0 \\ \kappa_i e_{i+1}, & else \end{cases} \tag{21}$$

where κ_i is a positive diagonal matrix. F_{Lds2} and Q_{Lds2} are described as,

$$\begin{aligned} F_{Lds2} &= -k_{2s1} e_2, k_{2s1} = \frac{1}{4\eta_1}(\gamma_{1M} + \|H_M\|\|\vartheta_1\|)^2 \\ Q_{Lds2} &= -k_{2s2} e_3, k_{2s2} = \frac{1}{4\eta_2}(\gamma_{2M} + \|\vartheta_{8M}\|\|\vartheta_2\|)^2 \end{aligned} \tag{22}$$

where H_M means that each term in the matrix take the maximum value. η_1 and η_2 are constants that fit the following robust condition,

$$e_2(\frac{\partial X_L}{\partial q} F_{Lds2} - \gamma_1) \le \eta_1,\ e_3(\frac{\partial X_L}{\partial q} Q_{Lds2} - \gamma_2) \le \eta_2 \tag{23}$$

3.2 Parameter estimation

Since one of the main objectives of this paper is to accurately estimate the mass the the end load, a first-order differentiation device is proposed. Two intermediate matrixes are designed as follows,

$$\delta_{si} = -\bar{\Phi}_i^T \vartheta_{si},\ \delta_{s1} = \frac{\partial X_L}{\partial q} F,\ \delta_{s2} = Q_L - \frac{\partial X_L}{\partial q}\lambda_A \dot{q} \tag{24}$$

Differentiate both sides of Eq.24 simultaneously, we have

$$\delta_{sif} = -\bar{\Phi}_{if}^T \vartheta_{si},\ \hat{\delta}_{sif} = -\bar{\Phi}_{if}^T \hat{\vartheta}_{si},\ \varepsilon_i = \hat{\delta}_{sif} - \delta_{sif} = -\bar{\Phi}_{if}^T \tilde{\vartheta}_{si},\ i = 1,2 \tag{25}$$

where ε_i is the error of intermediate matrixes. Then, the projective law is eventually generated as shown in Eq.26,

$$\dot{\Psi}_i = \begin{cases} \alpha_i \Psi_i - \zeta_i \Psi_i \bar{\Phi}_{if} \bar{\Phi}_{if}^T \Psi_i, & if\ \Lambda_{imax}(\Psi_i(t)) \le \rho_{iM} \\ 0, & othrewise \end{cases}, i = 1,2 \tag{26}$$

where $\zeta_i = (1 + v_i \Phi_{if}{}^T \Psi_{if} \Phi_i)^{-1}$, $\Lambda = \min\{2k_2 / \vartheta_{1\max}, 2k_3 / \vartheta_{8\max}\}$, v_i is a positive parameter and ρ_{iM} the upper bound of Ψ_i. α_i is the forgetting factor which partly determines the speed of the parameter adaptation. In this paper, this figure will be set to be a comparatively large value.

The adaptive law for unknown parameters is as follows,

$$\dot{\hat{\vartheta}}_{si} = Proj_{\hat{\vartheta}}(\Psi_i \tau),\ \tau = \zeta_i \Phi_{if} \varepsilon_i \tag{27}$$

where Ψ_i is a positive-definite matrix and determines the speed of parameter estimation. For this least square adaptive law, each term of Ψ_1 has an impact on the estimation speed of m_t. In order to estimate m_t as quickly and stably as possible, the value of Ψ_1 should be carefully adjusted and should be as large as possible.

Eq.27 will be used to update $\vartheta_1 = m_t$, the accuracy and speed of the adaptation will be attested in the next section.

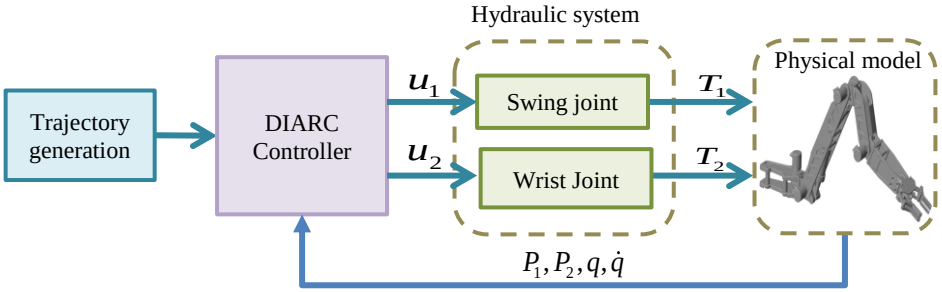

Fig. 3. Scheme diagram of simulation

4 Simulation setup and results

4.1 Simulation setup

A simulation is conducted using MATLAB Simulink. The scheme diagram of the simulation system is shown in Fig.3, and the picture of the manipulator can be seen in Fig.4. The physical model of the manipulator is built by Simscape Multibody, which takes the joint coupling into consideration. The trajectory generator can generate the

required trajectory, which is third-order differentiable. To simplify the simulations, both joints run the same P2P trajectory as shown in Fig.5. The sensor noise amplitude is set to 5×10^{-5} radians.

The simulation selected three groups for comparison, 1) PID controller, 2) DIARC controller without end load compensation, 3) DIARC with end load compensation.

The manipulator is installed with a 3kg end load, and the tracking accuracy of the three groups is compared first. Afterwards, the end load of the manipulator is changed to detect whether DIARC with end load compensation can accurately perceive the mass of the end load. The end load will be set as 0kg, 2.5kg, 5kg, 7.5kg and 10kg.

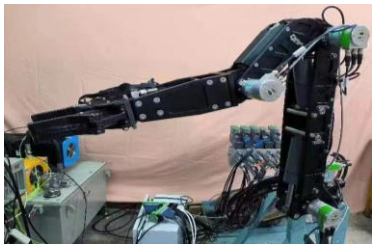

Fig. 4. The analyzed hydraulic manipulator

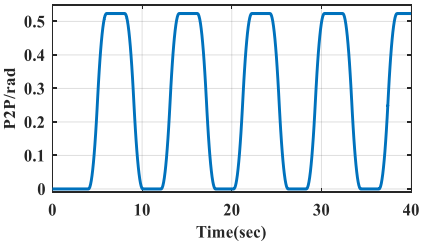

Fig. 5. Trajectory used in simulation

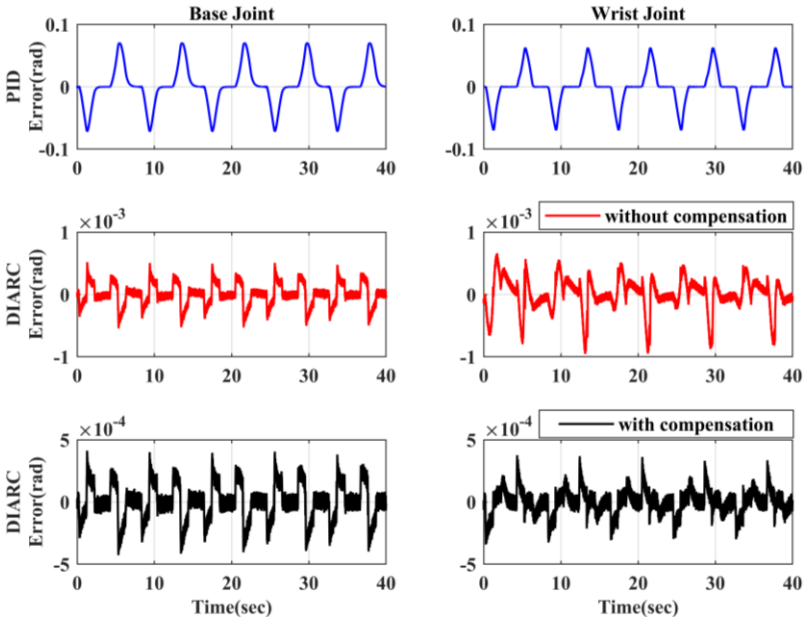

Fig. 6. Angular error of each joint with different controllers

4.2 Simulation results

In the simulation, a spherical weight of 3kg is placed in the gripper of the wrist joint, 0.4m away from the joint rotation axis. Under certain circumstances, the error curves

of each joint using the three kinds of controllers are shown in Fig.6. The tracking accuracy of the proposed DIARC controller has been significantly improved. The PID controller does not consider the complex dynamics of the hydraulic system. The error of each joint reached 0.06 rad. DIARC controller achieved far better control performance. The error of swing joint by DIARC controller without end load compensation is between -5.5×10^{-4} and 5.5×10^{-4} rad. Wrist joint error is between -1×10^{-3} and 6×10^{-4} rad. When the acceleration of the angle approaches the extreme value, there is a spike in tracking error due to the influence of the end load. Evidently, this is significantly reduced by DIARC with end load compensation. Due to the precise estimation of the end load, the calculation of the moment of inertia of the swing joint is also more accurate, which improves its tracking accuracy to a certain extent. The error of swing joint is between -4×10^{-4} and 4×10^{-4} rad, improved by 27%. The error of wrist joint is between -3×10^{-4} and 4×10^{-4} rad. The error amplitude has been significantly reduced by 56.3%.

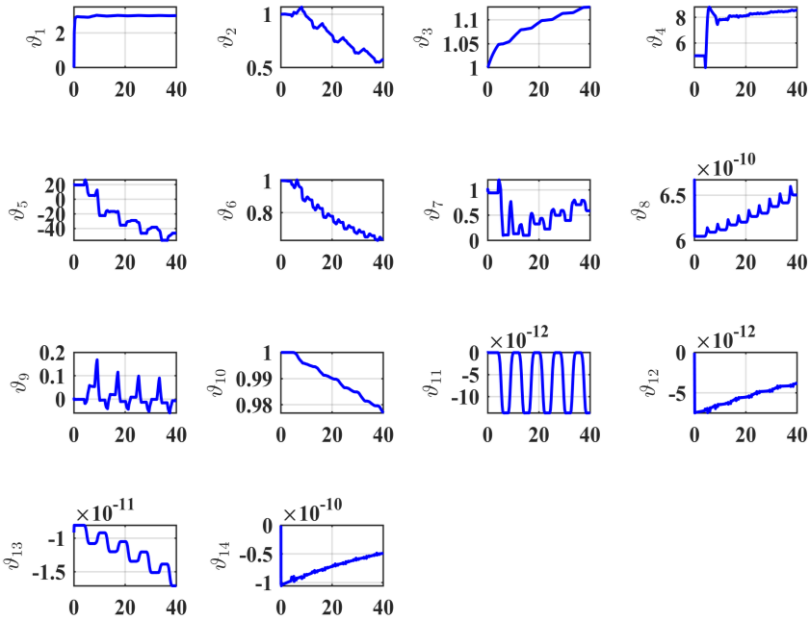

Fig. 7. Adaptive curves for each unknown parameter

The adaptive curves for each unknown parameter are shown in Fig.7. Each of the parameters tend to converge to a certain value which can be regarded as the real value. It can be found that the DIARC controller has the ability to accurately estimate unknown parameters. Therefore, the controller has the potential to accurately estimate the mass of the end load.

The end load of the manipulator is also estimated. A spherical weight is installed at the same location, but its weight is variable. Fig.8 shows the adaptive curve with five sets of end masses. The result indicate that the controller can quantitatively estimate the weight of the end load. More accurate data can be found in Table 1. It can be seen that

the controller has a high accuracy in estimating the end load. At the same time, due to the emphasis on improving the speed of end load adaptation in the early design, it only takes about 1s to obtain comparative accurate estimation of the load.

Table 1. Comparison of real and estimated weight

No.	Real value(kg)	Estimated value (kg)	Error (kg)
1	0	0.005	0.005
2	2.5	2.496	0.004
3	5	4.995	0.005
4	7.5	7.493	0.007
5	10	9.988	0.012

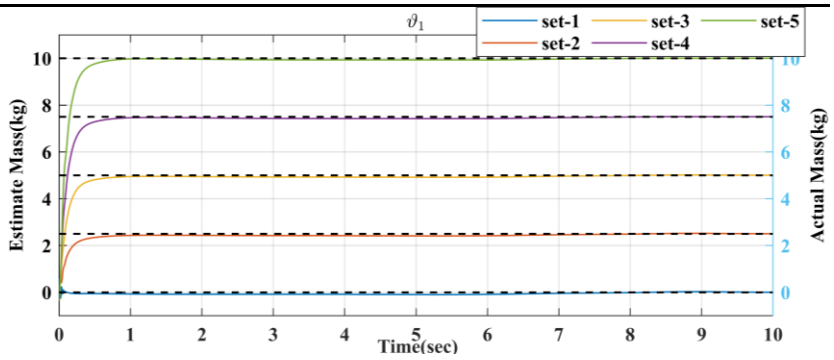

Fig. 8. The adaptive curves of end load

5 Conclusions

This developed a direct/indirect adaptive robust controller (DIARC), which can compensate for the influence of the end load on hydraulic manipulators and can effectively estimate the mass of the end load. Besides, the end load of hydraulic manipulator can be estimated online. Then, a co-simulation method is developed using MATLAB Simulink and Simscape to test the effectiveness of this controller. The maximum error of the swing joint and the wrist joint is only 73% and 43.7% of that of a conventional DIARC controller, respectively. At the same time, the controller also has high accuracy in estimating the end load, with the estimation error being only 0.012kg when the actual load is 10kg. The controller can effectively compensate for the additional torque caused by the gravity of the end load and the tracking accuracy is significantly enhanced. This proves potential of the DIARC controller proposed in this paper, which has a high guiding effect on industrial production.

Acknowledgement

This work is supported by National Natural Science Foundation of China (Nos. 52075476), Zhejiang Provincial Natural Science Foundation of China (No.

LR23E050001), and Fundamental Research Funds for the Central Universities (226-2023-00029).

References

1. Hu, J., Li, C., Chen, Z., Yao, B.: Precision motion control of a 6-dofs industrial robot with accurate payload estimation. IEEE/ASME Transactions on Mechatronics 25(4), 1821–1829 (2020).
2. Huang, Y., Pool, D. M., Stroosma, O., Chu, Q.: Long-stroke hydraulic robot motion control with incremental nonlinear dynamic inversion. IEEE/ASME Transactions on Mechatronics 24(1), 304-314 (2019).
3. Yao, J., Deng, W., Jiao, Z.: RISE-based adaptive control of hydraulic systems with asymptotic tracking. IEEE Transactions on Automation Science and Engineering 14(3), 1524-1531 (2017)
4. Yao, Z., Yao, J., Sun, W.: Adaptive RISE control of hydraulic systems with multilayer neural-networks. IEEE Transactions on Industrial Electronics 66 (11), 8638-8647 (2019).
5. Xia, Y., Nie, Y., Chen, Z.: Motion control of a hydraulic manipulator with adaptive nonlinear model compensation and comparative experiments. Machines 10(3), 214 (2022).
6. Koivumäki, J., Mattila, J., Stability-guaranteed impedance control of hydraulic robotic manipulators. IEEE/ASME Transactions on Mechatronics 22(2), 601-612 (2017).
7. Koivumäki, J., Mattila, J.: Stability-guaranteed force-sensorless contact force/motion control of heavy-duty hydraulic manipulators. IEEE Transactions on Robotics 31(4), 918–935 (2015).
8. Soewandito, D. B., Oetomo, D., Ang M. H.: Neuro-adaptive motion control with velocity observer in operational space formulation. Robotics and Computer Integrated Manufacturing 27(4), 829-842 (2011).
9. Bu, F., Yao, B.: Nonlinear model based coordinated adaptive robust control of electro-hydraulic robotic manipulators: methods and comparative studies. Engineering.purdue.edu 4, 3459-3464 (2000).
10. Liu, Y. F., Dong, M.: Research on adaptive fuzzy sliding mode control for electro-hydraulic servo system. Proceedings of the CSEE 26(14), 140-144 (2006).
11. Zhu, W. H., Dupuis, E., Piedboeuf, J.-C.: Adaptive output force tracking control of hydraulic cylinders. In: Proceedings of the 2004 American Control Conference, pp. 5066-5071. Boston, MA, USA (2004).
12. Kamezaki, M., Iwata, H., Sugano, S.: Condition-based less-error data selection for robust and accurate mass measurement in large-scale hydraulic manipulators. IEEE Transactions on Instrumentation and Measurement 66(7), 1820-1830 (2017).
13. Duan, S., Chen, L., Ma, Z., Lu, G.: Variable structure control with feedforward compensator for robot manipulators subject to load uncertainties. In: 2010 11th International Conference on Control Automation Robotics & Vision, pp. 2367-2372. Singapore (2010),
14. Zeng, A., Song, S., Lee, J. Rodriguez, A., Funkhouser, T.: TossingBot: Learning to throw arbitrary objects with residual physics. IEEE Transactions on Robotics 36(4), 1307-1319 (2020).
15. Colomé, A., Pardo, D., Alenyà G., Torras, C.: External force estimation during compliant robot manipulation. In: 2013 IEEE International Conference on Robotics and Automation, pp. 3535-3540. Karlsruhe, Germany (2013).